  Bull. Chem. Soc. Jpn., 57, 1760—1765 (1984) [Vol. 57, No. 7

Electron Spin Distributions and g-Value Shifts in the Novel Electron Donors with 1,3-Dithiole Rings

Atsushi TERAHARA,* Hiroaki OHYA-NISHIGUCHI, Noboru HIROTA, Hiroshi AWAJI,† Tokuzo KAWASE,† Shigeo YONEDA,† Toyonari SUGIMOTO,† and Zen-ichi YOSHIDA†

Department of Chemistry, Faculty of Science, Kyoto University, Kyoto 606

†*Department of Synthetic Chemistry, Faculty of Engineering, Kyoto University, Kyoto 606*

(Received December 22, 1983)

The ESR spectra of the cation radicals of TTF and its related compounds in which two 1,3-dithiole rings are connected by conjugated carbon and cumulene chains are measured. The spin distributions obtained from the *hfcc* due to the protons and sulfur atoms agree well with the results of the MINDO/3 calculations. The spin densities on the sulfur and central carbon atoms decreases as the central chain length increases. A linear relationship, $g=2.00379+0.00108\ a(S)$, between the *g*-values and the sulfur *hfcc* is noted and explained in terms of the Stone's theory. The *g*-values of the cation radicals with cumulene chains deviate from this relation and a possible cause is suggested.

The cation radical states of π electron donors play essential roles in making the organic metals such as tetrathiafuluvalene-tetracyanoquinodimethan(TTF-TCNQ) highly conductive[1] or in producing superconductivity in the salts of tetramethyltetraselenafuluvalene $(TMTSF)_2^{+\cdot}X^-(X^-=PF_6^-,\ ClO_4)$.[2] In order to understand the electronic band structures and the conduction mechanisms of these salts, it is desirable to know the details of the wave function and the orbital energies of the highest occupied molecular orbitals (HOMO). Electron spin resonance (ESR) and cyclic voltammetry measurements can provide information about them.

We have synthesized the compounds **2** to **5** shown in Fig. 1 in order to find electron donors better than TTF (**1**) and investigated their properties with various experimental techniques.[3] From the cyclic voltammetry measurements it was found that all these compounds have oxidation potentials ($E_{1/2}°$) lower than TTF and that they can be novel electron donors. Here we have studied the cation radicals of these compounds by ESR and examined the results in comparison with those predicted by the MINDO/3 calculation.

In this paper we first describe the results of the ESR investigation on the cation radicals of these compounds **1** to **5** in solution. From the hyperfine coupling constants (*hfcc*) of protons and sulfur atoms (^{33}S isotopes), the spin density distributions of the HOMO are determined in detail. The ESR spectra of the cation radicals of the several derivatives of **1**—**5** shown in Fig. 1 are also studied to examine the effects of substitution on the spin distributions.

Secondly, we compare the spin distributions obtained by ESR measurements with those calculated by the MINDO/3 method. We discuss how the HOMO changes as the central carbon chain in TTF becomes longer with conjugated or cumulene groups. In the case of **3**, there is an ambiguity whether the structure is *cis*- or *trans*-conformer. We investigated the compounds **6** and **7** shown in Fig. 1 in order to answer this question.

Finally, we discuss the relationship between the *g*-values and the sulfur *hfcc* noted for a series of compounds **1** to **3** using the Stone's theory. The *g*-values of **4** and **5**, however, deviate from this relationship. The origin of this deviation is discussed.

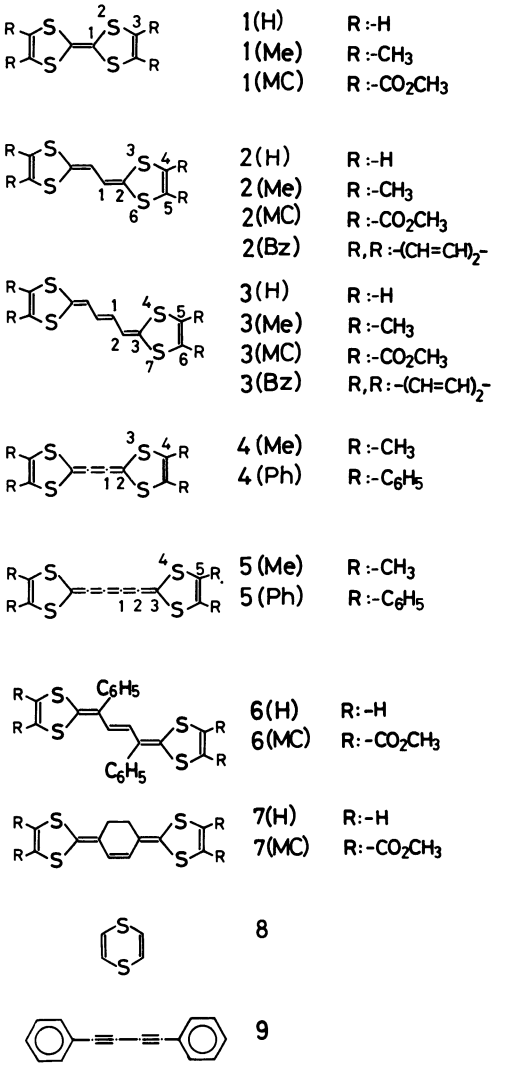

Fig. 1. Molecular structures investigated. The numbers distinguish the π-system and its derivatives are denoted by their abbreviations in last parenthes.

Experimental

The synthesis of the compounds **2**, **3**, and their derivatives was described elsewhere.[3] The series of compounds with cumulene skeletons are very unstable in the neutral states and we have not yet succeeded in synthesis. However the dication states of their tetramethyl and tetraphenyl derivatives are stable enough to be obtained in the form of perchlorate salts $\mathbf{4}^{2+}$ $2ClO_4^-$ and $\mathbf{5}^{2+}$ $2ClO_4^-$.[4] The generation of the cation radicals and the ESR measurements were carried out by using an electrochemical ESR system based on a JEOL-FE3X spectrometer.[5] The cation radicals of **1**, **2**, and **3** were generated by one-electron oxidation, while those of **4** and **5** were obtained by one-electron reduction of corresponding dications. Dry dichloromethane of spectroscopic grade was used as the solvent and tetrabutylammonium tetrafluoroborate was used as the supporting electrolyte. Potassiumn nitrosilbis(sulfate) was used as a standard sample for calibration of the magnetic field, the accuracy being within ±0.005 G†. *g*-Values were measured in reference to the signal of Cr(III) diluted in MgO (g=1.9800), the accuracy being within ±0.0001.

Results and Discussion

The ESR Spectra of $\mathbf{1}^{+\cdot}$, $\mathbf{2}^{+\cdot}$, *and* $\mathbf{3}^{+\cdot}$. The cation radicals of **1**(H), **2**(H), and their derivatives are stable but that of **3**(H) is a little unstable when it is oxidized at room temperature. The ESR spectra of these compounds do not change over the entire range of the temperature from −80 °C to room temperature. The proton *hfcc* and *g*-values of the cation radicals of **1**(H) and **1**(Me) are very close to those reported previously.[6] The ESR spectra of compounds $\mathbf{2}(H)^{+\cdot}$ and $\mathbf{3}(H)^{+\cdot}$ are shown in Figs. 2a and 3a, respectively, as examples. All of these ESR spectra have the linewidths of about 0.2 G and are easily analyzed and reconstructed by computer simulation (Figs. 2b and 3b).

The *hfcc* due to the isotopic sulfur atoms, ^{33}S (I= 3/2) were observed as satellite lines in some cases. Especially, in the case of tetrakis (methoxycarbonyl) derivatives of $\mathbf{2}(MC)^{+\cdot}$ and $\mathbf{3}(MC)^{+\cdot}$, it was easy to observe the ^{33}S satellites because of the simplification of the ESR spectra by methoxycarbonyl substitution. As a typical example, the satellite lines of $\mathbf{2}(MC)^{+\cdot}$ are shown in Fig. 4. Two kinds of ^{33}S satellites are expected for **2** and **3** from the molecular symmetries, but only one is expected in **1** because four sulfur atoms are equivalent. Two kinds of ^{33}S satellites were observed for most of **2** and **3** as expected. In the spectrum of $\mathbf{2}(H)^{+\cdot}$, however, only one ^{33}S satellite (3.98 G) was resolved because the ^{33}S satellite due to the *hfcc* smaller than 3.98 G overlapps with the other lines.

In Table 1 are listed the obtained *g*-values and the *hfcc* of the protons and ^{33}S. The assignment of the

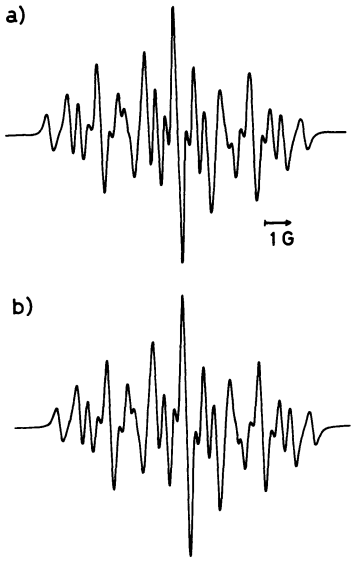

Fig. 2. The observed (a) and simulated (b) ESR spectra of $\mathbf{2}(H)^{+\cdot}$.

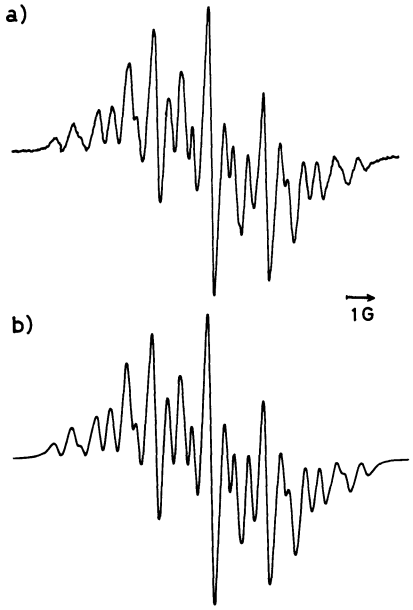

Fig. 3. The observed (a) and simulated (b) ESR spectra of $\mathbf{3}(H)^{+\cdot}$.

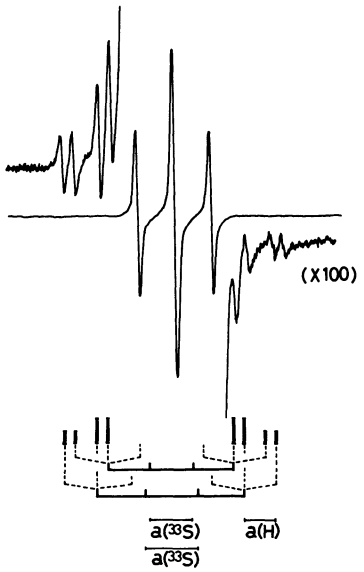

Fig. 4. The main splitting and ^{33}S satellite lines observed for $\mathbf{2}(MC)^{-\cdot}$; the analysis of the satellite lines indicated lower.

† 1 G=10^{-4} T.

hfcc due to protons and ^{33}S is based on the results of MINDO/3 calculation. Comparing the *hfcc* due to the central protons and the ^{33}S and the *g*-values of derivatives with those of the parent compounds, it is found that there is no substantial effect of substitution by tetramethyl, tetrakis(methoxycarbonyl), and dibenzo groups on the spin distribution. This is because the spin densities on the carbon atoms attached by substituent groups are relatively small. It is also noticeable that both the *g*-values and ^{33}S *hfcc* decrease in the order of **1**, **2**, and **3**. The same trend holds for the *hfcc* of the side protons and the central protons in **2** and **3**.

The ESR Spectra of $4^{+\cdot}$ *and* $5^{+\cdot}$. $4(Me)^{+\cdot}$ and $5(Me)^{+\cdot}$ are stable when they are generated by one-electron reduction at the temperature below −40 °C. The ESR spectrum of $4(Me)^{+\cdot}$ shown in Fig. 5a indicates a clear splitting of 0.69 G due to the twelve methyl protons, while in the spectrum of $5(Me)^{+\cdot}$ shown in Fig. 5b only a sign of about 0.5 G splitting due to the methyl protons is observed. The satellite ^{33}S splittings of $4(Me)^{+\cdot}$ and $5(ph)^{+\cdot}$ were observed but that of $5(Me)^{+\cdot}$ was not observed because of low intensity of the ESR signal. The four sulfur atoms are all equivalent in **4** and **5**.

Comparing the *hfcc* due to the methyl protons of $4(Me)^{+\cdot}$ and $5(Me)^{+\cdot}$ and the *hfcc* due to ^{33}S of $4(Me)^{+\cdot}$ and $5(Ph)^{+\cdot}$ with those of $1(Me)^{+\cdot}$, it is seen that the *hfcc* also decrease in the order of **1**, **4**, and **5**, as observed in the series of **2** and **3**. On the other hand, the *g*-value does not follow the same order. This point will be discussed later in detail.

Comparison with MO Calculation. We calculated the spin density distributions of these compounds using the MINDO/3 method which is capable of handling sulfur atoms.[7] The atomic coordinates of **1** were taken from the crystallographic data of $1(H)$[8] and those of the other compounds **2** to **5** were obtained based on the structure of **1** by using the bond lengths and bond angles adopted widely. For the methyl derivatives we carried out the calculation by fixing configurations of the methyl groups.

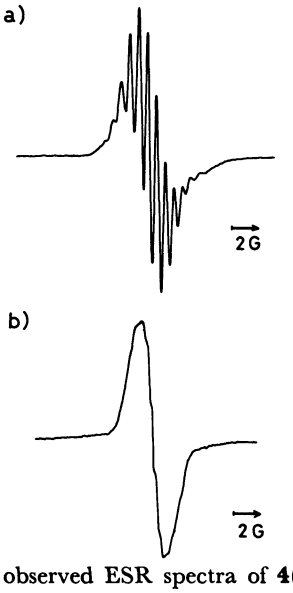

Fig. 5. The observed ESR spectra of $4(Me)^{+\cdot}$ (a) and $5(Me)^{+\cdot}$ (b).

The *hfcc* of the protons and ^{33}S obtained by the ESR study are compared with those estimated from the spin densities calculated by MINDO/3 method by using the following equations;

$$a(H) = -24.0 \cdot \rho(C) \quad \text{for aromatic protons,} \quad (1)$$

$$a(Me) = 507 \cdot \rho(H) \quad \text{for methyl protons,} \quad (2)$$

$$a(^{33}S) = 33.0 \cdot \rho(S) \quad \text{for } ^{33}S, \quad (3)$$

here $\rho(C)$ is the $2p\pi$ spin densities on the carbon atoms attached by the aromatic protons. For methyl protons $a(Me)$ are obtained from the averaged spin densities on the 1*s* orbitals of three methyl protons $\rho(H)$ by Eq. (2). The ^{33}S *hfcc* is estimated from the spin densities of $3p\pi$ of sulfur atoms $\rho(S)$ by using Eq. (3) proposed previousely.[9]

The calculated *hfcc* are also listed in Table 1. The correlation between the observed and calculated *hfcc* is shown in Fig. 6. From this figure it is seen that the agreement between the observed and calculated *hfcc* is satisfactory. We also note that there is a fair linear relationship between the calculated energy of the HOMO and the $E_{1/2}°$ measured by the cyclic voltammetry as shown in Fig. 7. Based on these results it is concluded that the HOMO calculated by the MINDO/3 method represents the actual orbital quite well.

The trend that the *hfcc* of ^{33}S and protons decrease in the order of **1**, **2**, and **3** is reproduced by this calculation. This trend is seen clearly from Fig. 8, which indicates the HOMO schematically. It is also seen from this picture that the spin is localized on the four sulfur atoms and central conjugated carbon chains. In the compounds with cumulene chains the situation is similar (Fig. 8), though the spin densities on the cumulene chains are slightly different from those on the normal conjugated chains.

The Structure of **3**. There are two possibilities for the structure of **3**, namely, *trans* and *cis* conformers. According to the chromatographic study, there is only one species for **3**. We tried to determine the structure of **3** by comparing the NMR and UV spectra of **3** with those of **6** and **7**, which are regarded as the rigid model compounds for the *trans* and *cis* forms of **3**, respectively. However, this attempt was in failure because there were no significant differences in the spectra between **6** and **7**. Then we compared the ESR parameters. It is also interesting to examine whether the spin density distribution changes by conformational change of *cis* and *trans* form, since the spin distribution in stilbene is known to depend on the conformation.[10]

The *hfcc* of both the central and side protons listed in Table 2 are almost the same for *trans* $6(H)^{+\cdot}$ and *cis* $7(H)^{+\cdot}$ (the difference between the two groups of the side protons was not seen in spectra). However the *g*-value of $6(H)^{+\cdot}$ is larger than that of $7(H)^{+\cdot}$ by 0.0004, which agree with the difference between $6(MC)^{+\cdot}$ and $7(MC)^{+\cdot}$. The *g*-value of $3(H)^{+\cdot}$ is very close to that of $6(H)^{+\cdot}$. Therefore, $3(H)^{+\cdot}$ is likely to be the *trans* form.

The Relationship Between The g-values and The ^{33}S

hfcc. As was described before, both the *g*-value and ^{33}S *hfcc* of the compounds **1**, **2**, and **3** decrease in the order of **1**, **2**, and **3**. Figure 9 shows the plots of the *g*-value *vs.* ^{33}S *hfcc* for all the compounds containing only C, H, and S atoms for which the ^{33}S splittings was observed in this study. The solid straight line obtained by a least square fit to the experimental points of five compounds is expressed by

$$g = 2.00379 + 0.00108 \cdot a(^{33}S) \quad (4)$$

The above relationship indicates that there is a linear

Table 1. The ESR parameters obtained in this study for the compounds **1** to **5** with the *hfcc* calculated by MINDO/3 method

Compound	$E_{1/2}°$/v	*g*-value	*hfcc*/G Obsd		Calcd	
1(H)	0.32	2.0084	1.26	(4H)	−0.99	(3)
			4.27	(^{33}S)	4.18	(2)
1(Me)	0.25	2.0081	0.78	(12H)	0.53	(3)
			3.99	(^{33}S)	4.06	(2)
1(Mc)	—	2.0081	4.52	(^{33}S)	—	
2(H)	0.24	2.0081	3.13	(2H)	−3.24	(1)
			1.23	(2H)	−0.78	(4)
			0.82	(2H)	−0.78	(5)
			3.98	(^{33}S)	3.62	(6)
					2.96	(3)
2(Me)	0.10	2.0072	2.90	(2H)	−3.10	(1)
			0.84	(6H)	0.42	(4)
			0.38	(6H)	0.36	(5)
				(^{33}S)	3.55	(6)
				(^{33}S)	2.91	(3)
2(Mc)	—	2.0080	2.93	(2H)		
			4.89	(^{33}S)		
			4.26	(^{33}S)		
2(Bz)	—	2.0076	2.92	(2H)	−3.13	(1)
			0.50	(2H)	−0.32	(8)
			0.28	(2H)	−0.26	(9)
			0.24	(4H)	−0.09	(10)
					−0.05	(7)
			4.07	(^{33}S)	3.59	(6)
			3.03	(^{33}S)	2.71	(3)
3(H)	0.26	2.0072	2.14	(4H)	−2.65	(2)
					−2.45	(1)
			0.99	(2H)	−0.57	(5)
			0.63	(2H)	−0.51	(6)
				(^{33}S)	2.81	(7)
				(^{33}S)	2.27	(4)
3(Me)	0.14	2.0070	2.32	(2H)	−2.56	(2)
			1.99	(2H)	−2.45	(1)
			0.99	(6H)	0.30	(5)
			0.33	(6H)	0.26	(6)
				(^{33}S)	2.80	(7)
				(^{33}S)	2.27	(4)
3(MC)	—	2.0072	2.21	(2H)		
			2.70	(^{33}S)		
3(Bz)	—	2.0067	2.10	(4H)		
4(Me)	0.09	2.0087	0.69	(12H)	0.40	(4)
			3.93	(^{33}S)	3.16	(3)
4(Ph)	—	2.0085	—		—	
5(Me)	−0.12	2.0066	0.5	(12H)	0.15	(5)
				(^{33}S)	3.16	(5)
5(Ph)	—	2.0053	3.69	(^{33}S)	—	

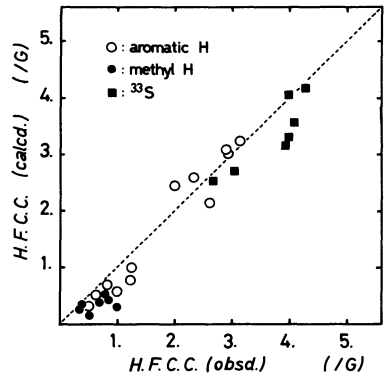

Fig. 6. The correlation between observed *hfcc* and calculated ones by MINDO/3 method for both protons and ^{33}S.

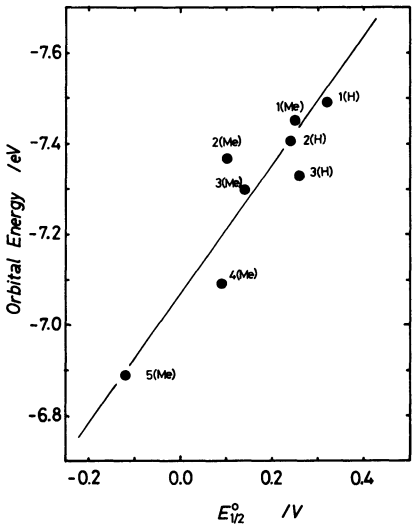

Fig. 7. The correlation between oxidation potentials ($E_{1/2}$) and calculated orbital energies of HOMO.

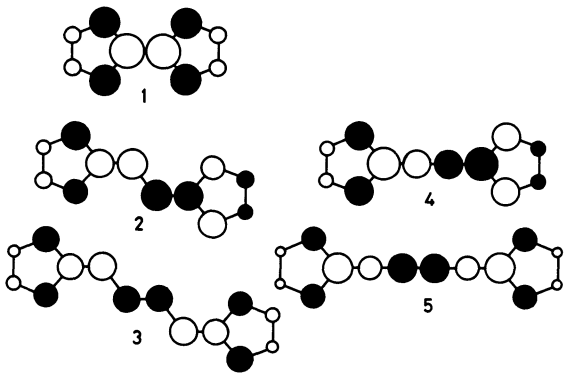

Fig. 8. Schematic view of the HOMO, the area of circle corresponds to the spin density and open circle indicates the positive sign of the coefficient of HOMO.

Table 2. The observed ESR parameters for **3**(H)$^{+\cdot}$, **6**(H)$^{+\cdot}$, **7**(H)$^{+\cdot}$, and their tetrakis(methoxycarbonyl) derivatives

	g-value	*hfcc*/G			*g*-value	*hfcc*/G	
3(H)	2.0072	2.14	(4H)	**3**(MC)	2.0072	2.21	(2H)
						1.78	(2H)
		0.99	(2H)				
		0.63	(2H)				
						3.19	(^{33}S)
						2.70	(^{33}S)
6(H)	2.0072	1.91	(2H)	**6**(MC)	2.0070	2.04	(2H)
		0.92	(4H)				
		2.66	(^{33}S)			2.96	(^{33}S)
						2.59	(^{33}S)
7(H)	2.0068	1.89	(6H)	**7**(MC)	2.0066	2.03	(2H)
						1.67	(4H)
		0.86	(4H)				
						2.89	(^{33}S)
						2.52	(^{33}S)

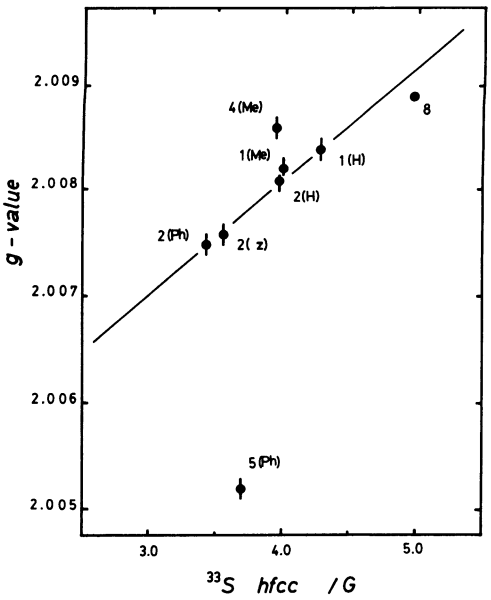

Fig. 9. The correlation between *g*-values and ^{33}S *hfcc* observed for the compounds containing only C, H, and S atoms. The solid line is a least square fitting line of Eq. (4) for five compounds without cumulene chain.

relation between the *g*-values and the π spin densities on the sulfur atoms. This means that the variation of the spin density on the sulfur atoms is the main cause of the *g* shift. In the following, we discuss this correlation by using the Stone's theory.[11]

One of the principal components of the *g* tensor can be derived by using the second order perturbation theory as

$$g^{\alpha\alpha} = g_e - 2\Sigma_n \frac{\langle \Psi_0 | \Sigma_\mu \zeta_\mu l_{\alpha\mu} | \Psi_n \rangle \langle \Psi_n | \Sigma_\nu l_{\alpha\nu} | \Psi_0 \rangle}{E_n - E_0}, \quad (5)$$

where the notations in Eq. 5 have usual meanings.[12] Stone[11] has shown that the deviation of *g*-value from the free electron *g*-value $\Delta g = g - g_e$ for the radicals of

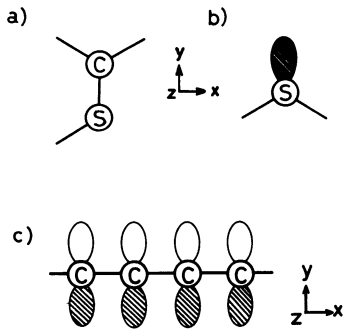

Fig. 10. The local axes for a) C–S bond, b) non-bonding orbital on sulfur atom, and c) cumulene or acetylene carbon chain. π orbital is along to z axis.

conjugated aromatic hydrocarbons can be expressed by the sum of the contributions from the σ-orbitals localized on C–C and C–H fragments. We formulate the contributions to Δg from the C–S fragment and nonbonding orbital on the sulfur atom in a similar way.

We first consider the contribution from the C–S bond. If the local axes are chosen as shown in Fig. 10a, bonding and antibonding orbitals of the C–S bond, $\psi(\sigma)$ and $\psi(\sigma^*)$, with the energy of E_σ and E_{σ^*}, respectively, can be written by linear combinations of two sp^2 orbitals belonging to the C and S atoms as

$$\psi(\sigma) = c_1\{\sqrt{1/3}\,S(\mathrm{C}) - \sqrt{2/3}\,P_y(\mathrm{C})\} + c_2\{\sqrt{1/3}\,S(\mathrm{S}) + \sqrt{2/3}\,P_y(\mathrm{S})\} \quad (6)$$

$$\psi(\sigma^*) = c_2\{\sqrt{1/3}\,S(\mathrm{C}) - \sqrt{2/3}\,P_y(\mathrm{C})\} - c_1\{\sqrt{1/3}\,S(\mathrm{S}) + \sqrt{2/3}\,P_y(\mathrm{S})\}. \quad (7)$$

Here, c_1 and c_2 are the normalization constants. On the other hand, the π orbital $\psi(\pi)$ (HOMO) with the energy E_π on the C–S fragment is expressd by

$$\psi(\pi) = c_C P_z(C) + c_S P_z(S), \quad (8)$$

where c_C and c_S are the coefficients of the singly occupied π orbital normalized over all atoms in the molecule. By substituting Eqs. (6), (7), and (8) to Eq. (5), we obtain

$$\Delta g^{xx} = \frac{4}{3}\frac{(c_1c_C - c_2c_S)(c_1\zeta_C c_C - c_2\zeta_S c_S)}{E_\pi - E_\sigma} + \frac{4}{3}\frac{(c_2c_C + c_1c_S)(c_2\zeta_C c_C + c_1\zeta_S c_S)}{E_\pi - E_{\sigma^*}}. \quad (9)$$

In order to simplify Eq. (9), we assume that $c_1 = c_2 = 1/\sqrt{2}$ and that the spin-orbit coupling constant of carbon atom ($\zeta_C = 29\,\mathrm{cm}^{-1}$) can be neglected compared with that of sulfur atom ($\zeta_S = 382\,\mathrm{cm}^{-1}$). Taking into account that c_C is the same order of magnitude as c_S and has an opposite sign to c_S in HOMO as seen in Fig. 8, we obtain the following simple relation between Δg^{xx} and c_S^2;

$$\Delta g^{xx} = \frac{4}{3}\frac{c_S^2\zeta_S}{E_\pi - E_\sigma} \quad (10)$$

Next, we treat the contribution from the non-bonding orbital on the S atom (Fig. 10b) in a similar way.

The non-bonding orbital on S atom, $\psi(n)$, with the energy of E_n is given by one of the three sp^2 orbitals;

$$\psi(n) = \sqrt{1/3}\,S(S) + \sqrt{2/3}\,P_y(S), \quad (11)$$

and we obtain the contribution for Δg^{xx} as well;

$$\Delta g^{xx} = \frac{4}{3}\frac{c_S^2\zeta_S}{E_\pi - E_n} \quad (12)$$

where, c_S^2 is the coefficient of $P_z(S)$ π orbital. The Δg due to the S atom is given after averaged for the three principal values as,

$$\Delta g = \frac{4}{9}\zeta_S\left(\frac{n_{C\text{-}S}}{E_\pi - E_\sigma} + \frac{n_S}{E_\pi - E_n}\right)c_S^2, \quad (13)$$

where $n_{C\text{-}S}$ and n_s represent the number of C–S bond and the number of non-bonding orbital, respectively.

Consequently, the g-value is expected to correlate with the spin density on the sulfur atom by Eq. (13). Here, the coefficient of c_S^2 corresponds to the slope of the straight line of Eg. (4). We can roughly estimate this coefficient to be 0.00136 by taking the energy differences to be 3 eV and 10 eV for $(E_\pi - E_n)$ and $(E_\pi - E_\sigma)$, respectively, and by converting the c_S^2 to $a(^{33}S)$ by Eg. (3). This value is in reasonable agreement with the value of 0.00108 obtained experimentally. On the other hand, the intercept of the line at $a(^{33}S)=0$ corresponds to the total contribution from the residual C–C and C–H fragments. The obtained intercept 2.00379 is close to the g-values of the radicals of aromatic hydrocarbons. Therefore, it is concluded that the main cause of the g shift in our case is attributed to the variation of the spin densities on the sulfur atom.

To examine the validity of our formulation further we plot the data for the cation radical of dithin (**8**) (g=2.0089; $a(^{33}S)$=9.84 G),[13] which has a very different π system from that of TTF. When we take account of the fact that there are only two sulfur atom in **8** instead of four in TTF, the correlation between g and $a(^{33}S)$ agrees with that predicted by the line in Fig. 9. This indicates that Eq. (13) is also applicable to other compounds with similar sigma structure.

The Anomaly in g*-Value of* $4^{+\cdot}$ *and* $5^{+\cdot}$. The plots of g-value *vs.* ^{33}S *hfcc* for $4(Me)^{+\cdot}$ and $5(ph)^{+\cdot}$ shown in Fig. 9 deviate from the correlation line; the g-value of $4(Me)^{+\cdot}$ is larger than the line by 0.0004 and that of $5(ph)^{+\cdot}$ is smaller by 0.0027. A similar decrease of the g-value was reported by Goldberg and Bard[14] in the case of the anion radical of 1,4-diphenyl-1,3-butadiyne (**9**); g=2.00216 is smaller than that of 1,4-diphenyl-1,3-butadiene anion radical by 0.00054 and smaller than g_e. They suggested that the cause of this decrease can be attributed to the decrease of the energy difference between the π_z-orbital and the lowest unoccupied π_y-orbital, the latter being localized on the central acetylene carbons and perpendicular to the π_z-orbital shown in Fig. 10c. The anomalous g shift in our case may also be explained in a similar way.

The contribution of the acetylene or cumulene carbon chain to the g shift can be calculated by Eq. (5) as follows. The π_y-orbitals are expressed by the linear combination of P_y orbitals;

$$\psi^{(n)}(\pi_y) = \Sigma_i b_i^{(n)} P_{yi}(C), \quad (14)$$

and the π_z-orbital (HOMO) is also expressed by

$$\psi(\pi_z) = \Sigma_i c_i P_{zi}(C) \quad (15)$$

Substituting Egs. (14) and (15) to Eg. (5), we obtain

$$\Delta g = \frac{2}{3}\zeta_C \Sigma_n \frac{\{\Sigma_i c_i b_i^{(n)}\}^2}{E_{\pi z} - E_{\pi y}^{(n)}}. \quad (16)$$

Small energy denominators in Eq. (16) lead to a large Δg.

Therefore, the anomaly in g-value of $4^{+\cdot}$ and $5^{+\cdot}$ are likely due to the closeness of π_y and π_z orbitals. We estimate the energy differences by using Eq. (16). If the Hückel orbitals of butadiene with β=2.5 eV are used for the energies and the coefficients $b_i^{(n)}$ of π_y-orbitals, the energy differences between the π_z-orbital and the lowest unoccupied π_y-orbital are estimated to be 0.026 eV and 0.26 eV for $5(ph)^{+\cdot}$ and $9^{-\cdot}$, respectively.

On the other hand, when the energy of the π_z-orbital is very close to the energy of the doubly occupied orbital of π_y-orbital, the g-value becomes large. The slightly large g-value of $4(Me)^{+\cdot}$ is considered to be due to this effect. The energy difference in $4(Me)^{+\cdot}$ is estimated to be 0.30 eV by a similar argument.

Investigation on the electronic conductivities of the organic metals containing radical cations of the present compounds are in progress.

References

1) J. P. Ferraris, D. O. Cowan, V. Walatka, Jr., and J. H. Perlstein, *J. Am. Chem. Soc.*, **95**, 948 (1973); L. B. Colemen, M. J. Cohen, D. J. Sandman, F. G. Yamagishi, A. F. Garito, and A. G. Heeger, *Solid State Commun.*, **12**, 1125 (1973).

2) K. Bechgaard, C. S. Jacobsen, H. J. Pedersen, and N. Thorup, *Solid State Commun.*, **33**, 1119 (1980); D. Jerome, A. Mazaud, M. Ribault, and K. Bechgaard, *J. Phys., Lett.*, 41, L95 (1980); K. Andres, F. Wudl, D. B. McWhan, G. A. Thomas, D. Nalewajek, and A. L. Stevens, *Phys. Rev. Lett.*, **45**, 1449 (1980).

3) Z. Yoshida, T. Kawase, H. Awaji, I. Sugimoto, T. Sugimoto, and S. Yoneda, *Tetrahedron Lett.*, **1983**, 3469; Z. Yoshida, T. Kawase, H. Awaji, and S. Yoneda, *ibid.*, **1983**, 3473.

4) Z. Yoshida, H. Awaji, T. Sugimoto, and S. Yoneda, in preparation.

5) H. Ohya-Nishiguchi, *Bull. Chem. Soc. Jpn.*, **52**, 2064 (1979).

6) S. Hunig, G. Kielich, H. Quast, and D. Scheutzow, Liebigs *Ann. Chem.*, **1973**, 310; F. Wudl, A. A. Kruger, M. L. Kaplan, and R. S. Hutton, *J. Org. Chem.*, **42**, 768 (1977).

7) R. C. Bingham, M. J. S. Dewar, and D. H. Lo, *J. Am. Chem. Soc.*, **97**, 1285 (1975).

8) W. F. Cooper, N. C. Kenny, J. W. Edmons, A. Nagel, F. Wudl, and P. Coppens, *Chem. Commun.*, **1971**, 889.

9) F. B. Bramwell, R. C. Haddon, F. Wudl, M. L. Kaplan, and J. H. Marshall, *J. Am. Chem. Soc.*, **100**, 4612 (1978).

10) F. Gerson, H. Ohya-Nishiguchi, M. Szwarc, and G. Levin, *Chem. Phys. Lett.*, **52**, 587 (1977).

11) A. J. Stone, *Mol. Phys.*, **6**, 509 (1963).

12) For Example, see N. M. Atherton, "Electron Spin Resonance, Theory and Applications,"John Wily and Sons Inc., p. 207 (1973).

13) P. D. Sullivan, *J. Am. Chem. Soc.*, **90**, 3618 (1968).

14) I. B. Goldberg and A. J. Bard, *Chem. Phys. Lett.*, **7**, 139 (1970).